Nationaal Lucht- en Ruimtevaartlaboratorium
National Aerospace Laboratory NLR

Executive summary

Modelling of Microstructure and Mechanical Property Changes in Gas Turbine Alloys

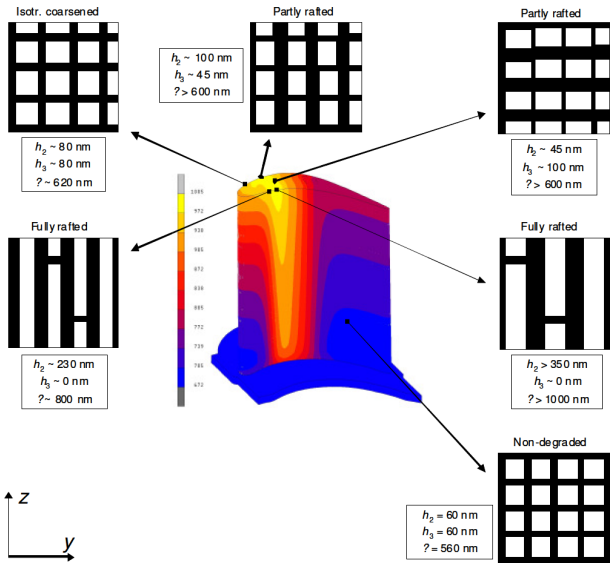

Report no.
NLR-TP-2010-379

Author(s)
A. Scholz
M. Nazmy
B. Fedelich
T. Tinga
R.A. Huls

Report classification
UNCLASSIFIED

Date
February 2011

Knowledge area(s)
Gasturbinetechnologie
Computational Mechanics and Simulation Technology

Descriptor(s)
Single Crystals
Creep Analysis
Micromechanics
Constitutive Equations
Nickel Alloys

Problem area
Superalloys are widely used as gas turbine blade materials because of their very high resistance against high temperature plastic deformation. The superior high temperature behaviour is attributed to the two-phase composite microstructure, consisting of a γ matrix containing a large volume fraction of cuboidal γ' particles. For both gas turbine component design and maintenance it is important to have the ability to perform a reliable life time assessment. To be able to accurately model the material behaviour, the two-phase nature of the superalloy must be taken into account.

Description of work
Two models were developed that incorporate the microstructure in a constitutive model for nickel based superalloys for use in a finite element package. The results of these models were compared with measurement of tensile, creep and fatigue properties. Furthermore, the models were applied to a complex geometry.

This report is based on a presentation held at the 9th Liège Conference on Materials for Advanced Power Engineering, Liège, Belgium, September 2010.

Results and conclusions
Two different models for incorporating microstructural details of nickel superalloys are available for finite element calculations. These models can predict the influence of microstructural degradation on creep and fatigue properties.

Applicability
The constitutive models can be used to predict creep and fatigue in high temperature gas turbine components.

Nationaal Lucht- en Ruimtevaartlaboratorium, National Aerospace Laboratory NLR

Anthony Fokkerweg 2, 1059 CM Amsterdam,
P.O. Box 90502, 1006 BM Amsterdam, The Netherlands
Telephone +31 20 511 31 13, Fax +31 20 511 32 10, Web site: www.nlr.nl

Nationaal Lucht- en Ruimtevaartlaboratorium
National Aerospace Laboratory NLR

NLR-TP-2010-379

Modelling of Microstructure and Mechanical Property Changes in Gas Turbine Alloys

A. Scholz[1], M. Nazmy[2], B. Fedelich[3], T. Tinga[4] and R.A. Huls

[1] Institut fuer Werkstoffkunde, TU Darmstadt

[2] ALSTOM Power

[3] BAM

[4] Netherlands Defence Academy

This report is based on a presentation held at the 9th Liège Conference on Materials for Advanced Power Engineering, Liège, Belgium, September 2010.

This publication has been refereed by the Advisory Committee AEROSPACE VEHICLES.

Customer	National Aerospace Laboratory NLR
Contract number	--
Owner	National Aerospace Laboratory NLR
Division NLR	Aerospace Vehicles
Distribution	Unlimited
Classification of title	Unclassified
	February 2011

Approved by:

Author	Reviewer	Managing department

Summary

High efficiency in gas turbines requires increased gas temperatures. Gas temperatures above 1100°C can only be handled using air cooled structures to keep the metal temperatures below 1000°C. Nickel-base single crystal (SX) superalloys have higher elevated temperature strength than conventionally or directionally cast superalloys. SX superalloys are therefore very attractive for use in aero engines and gas turbines as blade material since they allow higher operating temperatures. Within the Work Packages 3 & 4 of the COST 538 Action "Plant life extension" deformation and lifetime of SX alloy CMSX-4 using different material simulation concepts were in the focus. Of special interest are the efforts to incorporate degradation effects into the models. At first, two multi-scale models were developed for the purpose of connecting the macroscopic material behaviour to the microstructural composition of the material. The matrix and precipitate phase constitutive behaviour was considered. Formulations are based on the physical mechanisms acting on the microscopic level. The developed damage model combines creep-fatigue damage accumulation. Furthermore, the capability of the model to predict the effect of microstructural degradation on mechanical response was demonstrated by the simulation of experiments on degraded material. Moreover, a constitutive model demonstrates the potentiality to predict rafting in superalloys with large volume fraction of the γ' phase and its influence on the alloy strength. Hence it can be regarded as a candidate for use in structural analysis of blades in service conditions. Finally, the developed micro-structural based models have been successfully applied to an ex-service un-cooled blade i.e. a case study.

Content

Modelling of Microstructure and Mechanical Property Changes in Gas Turbine Alloys

Alfred Scholz *, Mohamed Nazmy **, Bernard Fedelich [x], Tiedo Tinga [+], Rob Huls [#)]
* Institut fuer Werkstoffkunde, Technische Universitaet Darmstadt, Germany
** ALSTOM Power, Baden, Switzerland, [x] BAM, Berlin, Germany
[+] Netherlands Defence Academy, Den Helder, The Netherlands
[#)] National Aerospace Laboratory, Emmeloord, The Netherlands

Abstract

High efficiency in gas turbines requires increased gas temperatures. Gas temperatures above 1100°C can only be handled using air cooled structures to keep the metal temperatures below 1000°C. Nickel-base single crystal (SX) superalloys have higher elevated temperature strength than conventionally or directionally cast superalloys. SX superalloys are therefore very attractive for use in aero engines and gas turbines as blade material since they allow higher operating temperatures.

Within the Work Packages 3 & 4 of the COST 538 Action "Plant life extension" deformation and lifetime of SX alloy CMSX-4 using different material simulation concepts were in the focus. Of special interest are the efforts to incorporate degradation effects into the models. At first, two multi-scale models were developed for the purpose of connecting the macroscopic material behaviour to the microstructural composition of the material. The matrix and precipitate phase constitutive behaviour was considered. Formulations are based on the physical mechanisms acting on the microscopic level. The developed damage model combines creep-fatigue damage accumulation. Furthermore, the capability of the model to predict the effect of microstructural degradation on mechanical response was demonstrated by the simulation of experiments on degraded material.

Moreover, a constitutive model demonstrates the potentiality to predict rafting in superalloys with large volume fraction of the γ' phase and its influence on the alloy strength. Hence it can be regarded as a candidate for use in structural analysis of blades in service conditions. Finally, the developed micro-structural based models have been successfully applied to an ex-service un-cooled blade i.e. a case study.

Keywords: Nickel base superalloys, Degradation, Modelling, Microstructure, Mechanical properties

1 Background

Gas turbines are extensively used for the propulsion of aircrafts and in power generation. Their most severely loaded parts, the turbine rotor blades, are manufactured from single crystal nickel-base superalloys. The superior high temperature behaviour of these materials is attributed to the two-phase composite microstructure of a γ-matrix consists of solid solution of Ni,Cr,W,Mo etc and a large volume fraction of the second phase precipitates of γ'- Ni_3 (Al,Ta). During service, the initially cuboidal precipitates evolve to elongated plates through a diffusion-based process called rafting. In order to include this deterioration process in the life assessment of gas turbine components, models must be

available to handle the specific microstructural changes and the corresponding mechanical behaviour.

The main objectives of the COST538 activities are the extension of the reliable lifetime of the critical components in the high temperature power plants. The corresponding components require detailed investigations of the degradation processes on the microstructure and the mechanical properties (**Figure 1**).

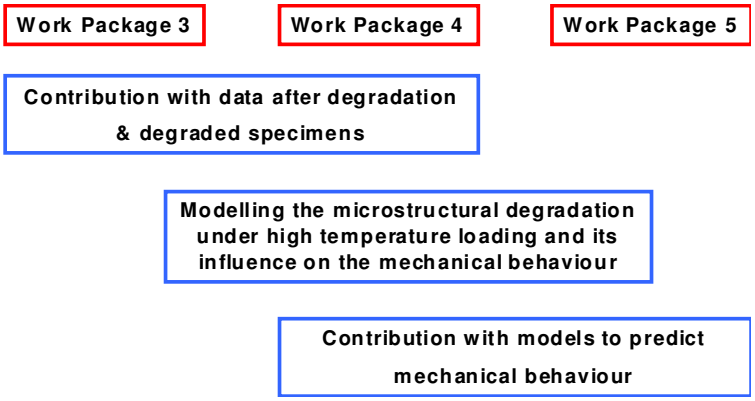

Figure 1: Illustration of interaction with Work Package 3 (material degradation), Work Package 4 (Modelling) and Work Package 5 (Case Studies)

In Work Package 4 of the COST 538 Action two models have been developed that incorporate the effect of microstructure degradation on the mechanical response (Work Package 3). In this paper the models developed by the Bundesanstalt für Material-forschung (BAM) and the National Aerospace Laboratory in cooperation with the Netherlands Defence Academy (NLR/NLDA) are introduced briefly with reference to extensive papers being available from the corresponding authors. Moreover, both models have been applied to predict the degradation and fatigue life of test specimens and real gas turbine components.

In order to establish the relationship between parameters relevant to application i.e. temperature, time & stresses and the mechanical properties experiments have been conducted. Microstructural investigations were performed to identify material model parameters.

Investigations reported here are focused on the crystallographic orientation <001>, which is the most relevant case. In addition the case <111> has also been investigated on the base of a limited amount of experiments.

2. Experimental

Test bars (20mm diameter, 160mm length) of alloy CMSX-4, orientation <001> were received from HOWMET, Exeter (Master heat: GE148, Cast 704P6253/9556). Chemical composition is given in **Table 1** [1].

Table 1: Chemical composition and heat treatment

Main alloying elements

	Cr	Ni	Co	Mo	W	Ta	Nb	Al	Ti	Re
Bar stock	6.4	bal	9.5	0.58	6.4	6.5	<0.01	5.7	1.06	2.8
Cast sample	6.3	bal	9.5	0.59	6.3	6.45	0.01	5.73	1.06	2.8

Residal elements

	C	B	Zr	Fe	Cu	Si	Mn	P	S	Hf	Pt	V
Bar stock	0.0043	<0.0020	0.0034	0.08	<0.005	<0.02	<0.01	<0.001	<0.0005	0.09	<0.05	<0.01
Cast sample	0.005	<0.002	0.0031	0.09	<0.005	0.02	<0.01	<0.001	<0.0005	0.1	<0.05	<0.01

Trace elements

(in ppm)	Bi	Tl	Ag	Pb	Te	Se	Sn	Ga	Mg	O2	N2
Bar stock	<0.1	<0.2	<0.5	<0.5	<0.2	<0.5	<10	<10	20	6	3
Cast sample	<0.1	<0.2	<0.5	<0.5	<0.5	<1	<10	<10	13	6	3

Heat treatment

SV6365	Proprietary cycle of three stages to give eutectic <3% maximum and <1% avarage of ten frames measured on Micro WF67

Chemical composition as well as the short term properties were in accordance with data from earlier batch of the same material [2]. The metallographic investigations showed typical microstructure in the as delivered condition as shown in (**Figure 2**).

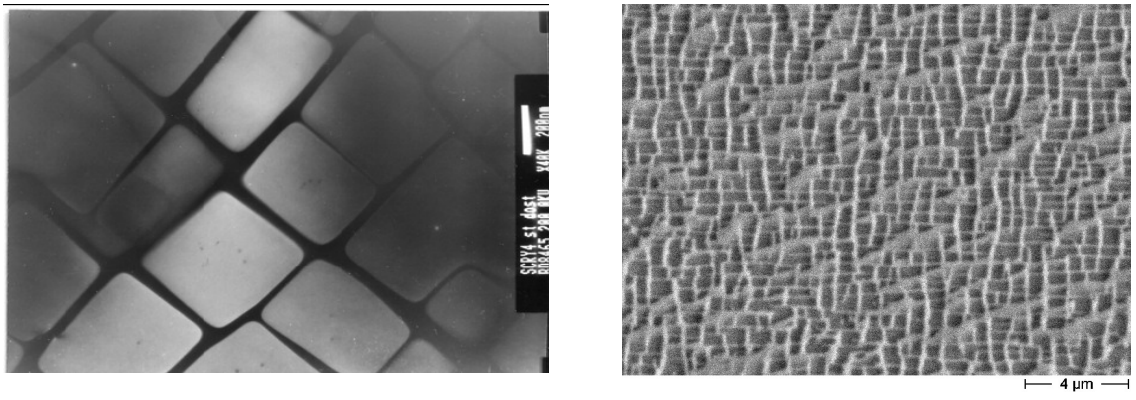

Figure 2: SEM dark field image of CMSX-4 microstructure (taken from γ' reflection), (left) & SEM image (right)

In order to investigate degradation effects, the underlying conditions were chosen as follows: 1050°C/115MPa/300h and 1050°C/68 MPa/2500 h. Tensile tests were conducted on samples which have been degraded. The degradation led to a significant drop in the 0.5% yield stress as given in (**Figure 3**). The results reported here have been partly published in earlier works [3] & [4].

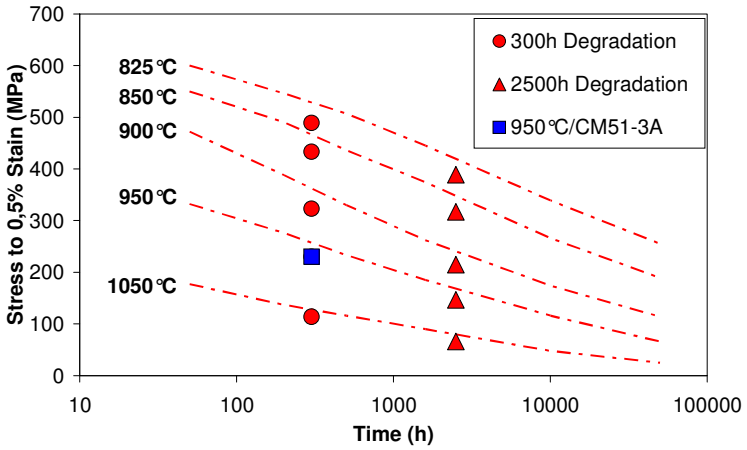

Figure 3: Reduction of tensile stresses to achieve 0.5% plastic strain at tensile testing (CMSX-4) with increase of degradation time

In order to achieve a temperature dependant overview of degradation, a series of tensile tests were performed at room temperatures to 950°C. A significant reduction in yield stress is observed throughout the investigated temperature range as shown in **Figure 4**. A remarkable influence of the effect of degradation on yield stress was observed at room temperature [3]. The results on ultimate strength also show a clear influence of the effect of degradation (**Figure 5**). Rupture elongation at room temperature is increased after degradation, while at elevated temperatures ductility is somewhat reduced (**Figure 6**).

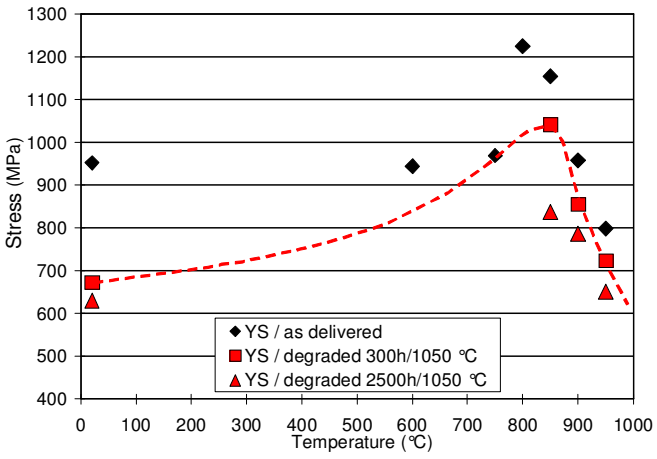

Figure 4: Yield stress vs. temperature at tensile testing and influence of degradation, CMSX-4, <001>

In summary, the degradation has a strong effect on yield stress at low temperatures. Figures **7-a, b & c** show fracture surface after testing at RT, microstructure of degraded specimen and a corresponding TEM micrograph of the dislocation structure of the tested

specimen. The γ' morphology also changed sligtly in comparison to the as delivered condition i.e. as in **Figure 2**.

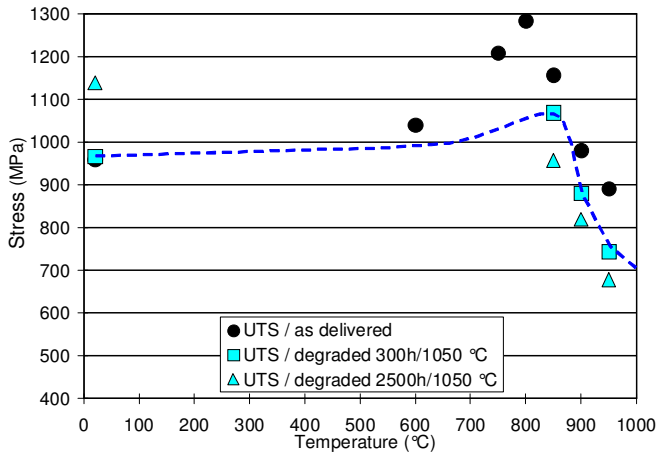

Figure 5: Ultimate strength vs. temperature at tensile testing and influence of degradation, CMSX-4 <001>

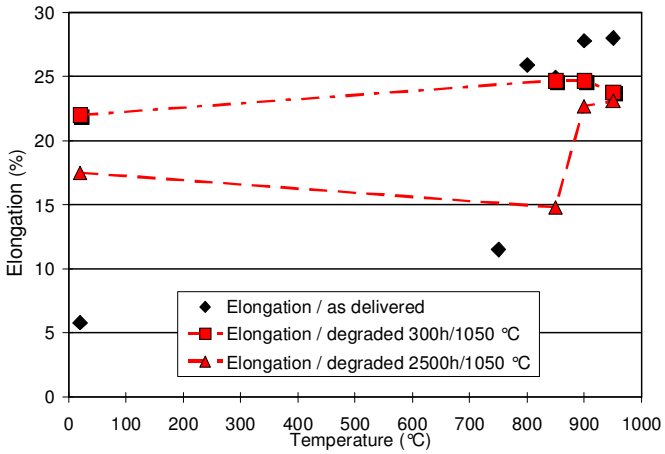

Figure 6: Rupture elongation vs. temperature at tensile testing and influence of degradation, CMSX-4 <001>

Figure 8 shows the shape of the specific creep specimen used to generate results on degradaded microstructures, at different stresses, required for the development of the degradation model presented in reference [6].

The changes in γ'-morphology were identified and illustrated in **Figure 9**. The rafting time, the corresponding stress, and temperature were plotted as shown in **Figure 8**. The γ'-morphological changes after degradation were used to develop the quantitative model for CMSX-4 [5].

Besides static loading, the degradation followed by cyclic loading is also of design relevance. A limited amount of fatigue experiments were performed at 950°C. **Figure 10** shows the results of a limited number of fatigue tests, performed at 950°C and a strain ratio R_ε = -1, illustrating the effect of degradation on low cycle fatigue (LCF). A

significant reduction of fatigue life, after degradation with the conditions 1050°C/ 68MPa/2500h, was observed in **Figure 10**. At a lower fatigue testing temperature e.g. 750°C, the fatigue life was also affected by degradation [1].

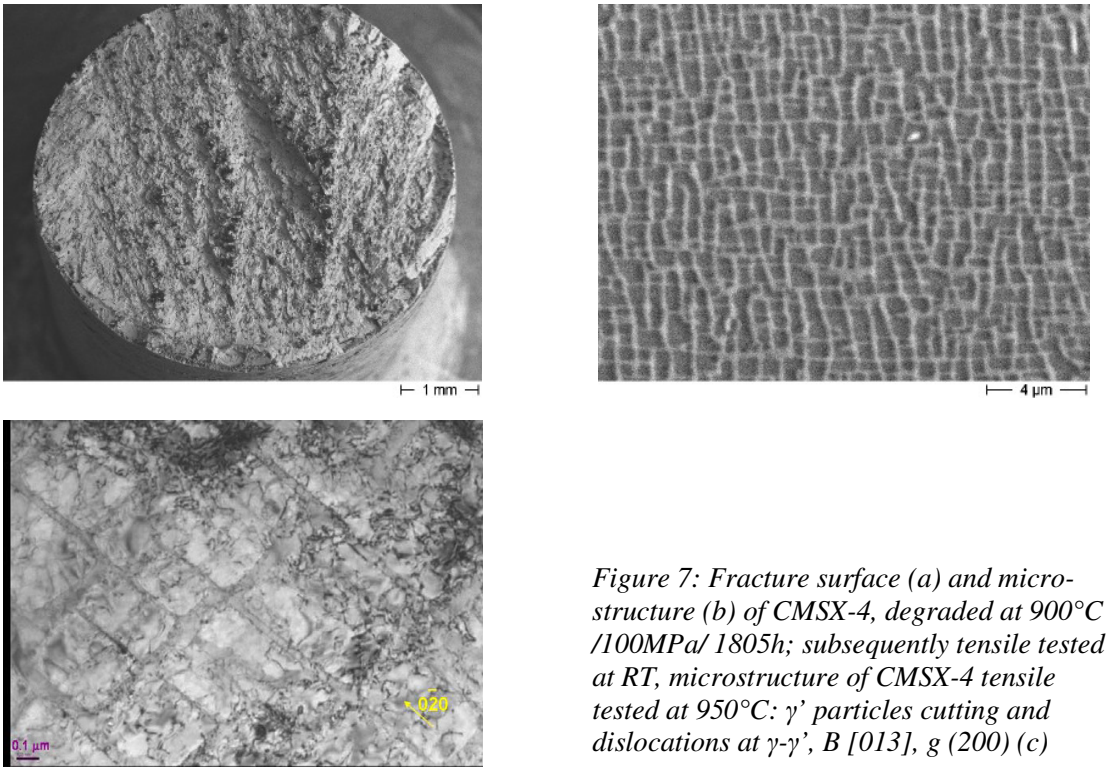

Figure 7: Fracture surface (a) and micro-structure (b) of CMSX-4, degraded at 900°C /100MPa/ 1805h; subsequently tensile tested at RT, microstructure of CMSX-4 tensile tested at 950°C: γ' particles cutting and dislocations at γ-γ', B [013], g (200) (c)

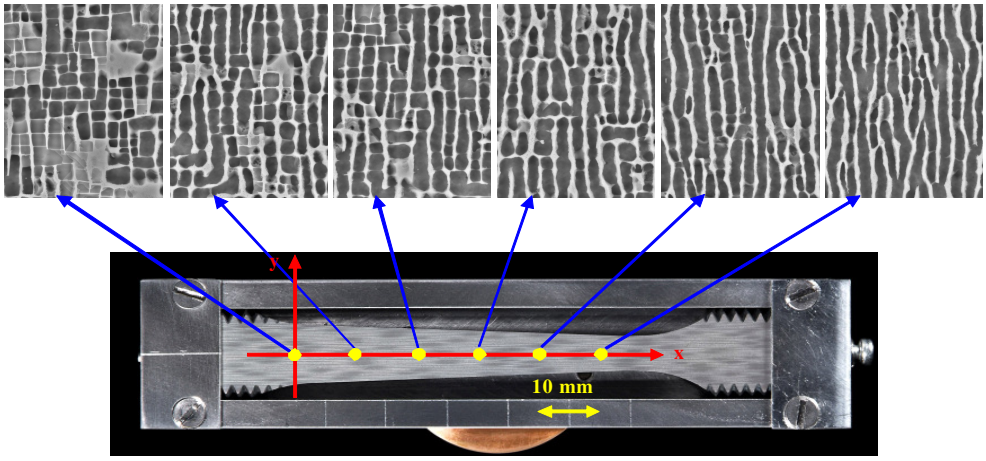

Figure 8: SEM holder with conical specimen degraded at 1050°C/175 h. Areas of analysis and SEM images correspond to the stress range 59 to 94 MPa [6]

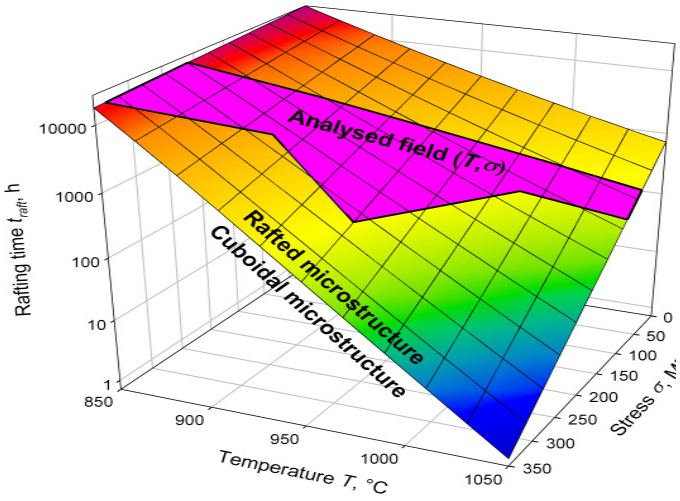

Figure 9: Time for complete raft formation as a function of temperature and stress. The field of degredation experiments is marked with the solid line [6]

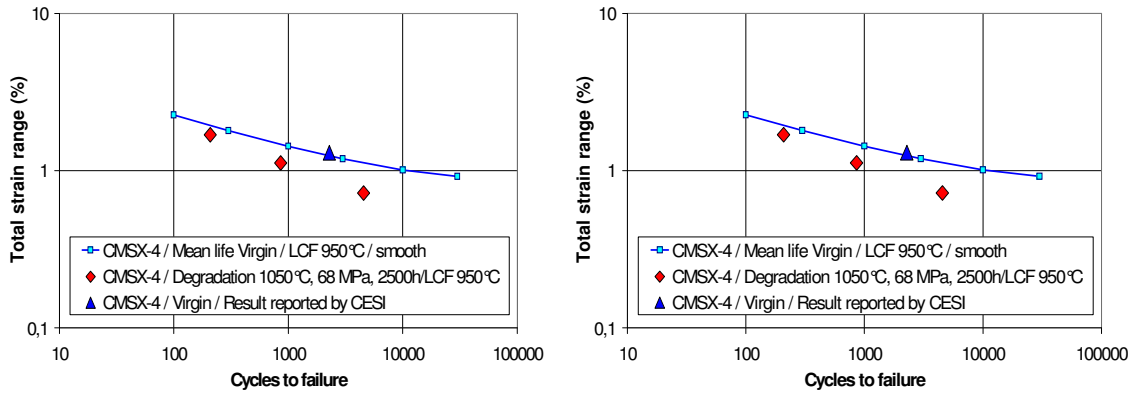

Figure 10: Reduction of fatigue life at 950°C (left) and 750°C (right) after degradation

In the following sections the two material models are presented. BAM has developed a model for microstructural degradation under high temperature loading and its influence on the mechanical behaviour while NLR / NLDA developed a "Multi-Scale Model" to connect macroscopic material behaviour to the microstructural changes of material.

In terms of material parameter identification, significant experimental results were made available by the partners of references [1], [2], [5] and [7] as shown for example in **Figure 11**. Creep data were contributed to identify the static recovery in the material model. The fatigue life behaviour of CMSX-4 has been described with a new temperature dependent approach. In addition, specific strain controlled cyclic relaxation experiments were performed. These experimental results were needed to model the kinematic hardening effects as shown in **Figure 12**.

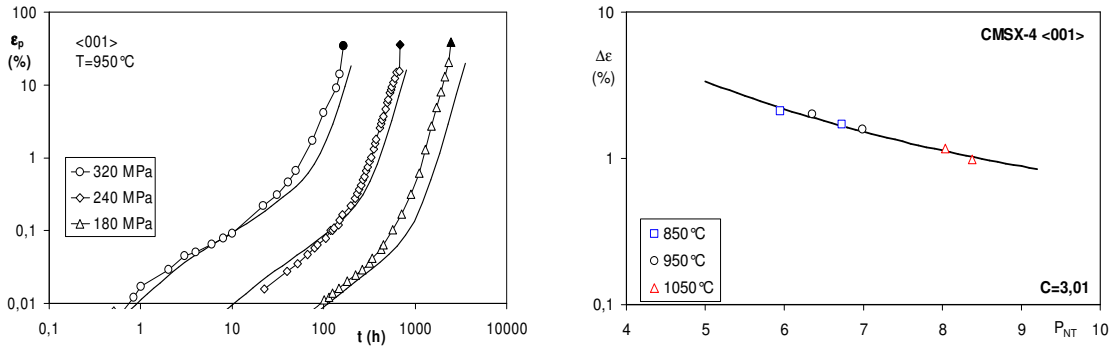

Figure 11: Creep behaviour of SX alloy CMSX-4 at 950°C, orientation <001>, modelling by Garofalo creep equation (left) and modelling of fatigue life by a temperature dependent approach, [2] (right)

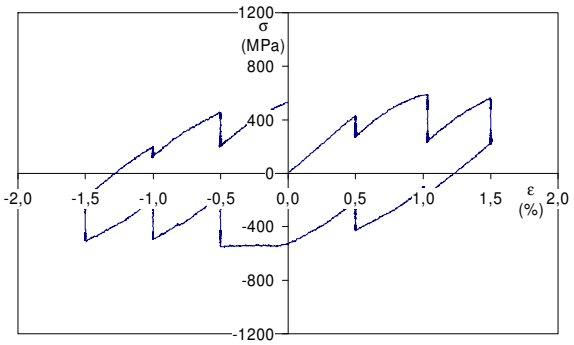

Figure 12: Symmetric tension and compression material behaviour at 950°C and low strain rate derived from cyclic stress relaxation experiments, CMSX-4 <001> [7]

3. BAM Constitutive Material Model

A constitutive material model with capacity to predict rafting in components has been developed and calibrated for the SX alloy CMSX-4. Herein, the microstructure influence is assumed to mostly depend on the channel width $w(t)$, which increases during creep due to two phenomena:

- the homothetic growth of γ'-precipitates, called isotropic coarsening,
- the coalescence of adjacent precipitates, called rafting.

In accordance, $w(t)$ varies between two time-dependent limits, which correspond to either the ideal cube or the infinite plate microstructure under isotropic coarsening. This evolution is shown in **Figure 13**.

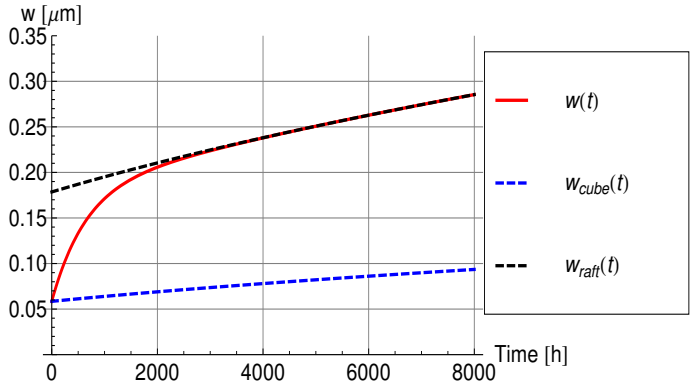

Figure. 13: Schematic evolution of the channel width between its two limits

The degree of rafting progress, as opposed to isotropic coarsening is defined by the variable

$$\xi = \frac{w - w_{cube}}{w_{raft} - w_{cube}}, \quad 0 \le \xi \le 1 \tag{1}$$

where w_{cube} and w_{raft} are the previously mentioned limiting cases of the microstructure. The microstructure dependent constitutive model has been presented in details in [5] [8]. It is based on crystal viscoplasticity for octahedral and cubic slip systems and on the assumption of thermally activated deformation mechanisms. In particular, the shear rate of the octahedral systems crucially depends on the Orowan stress τ^{Orowan}, which acts as a smooth threshold for yielding

$$\dot{\gamma}_g^o = \rho_g^o \; \sinh\left[\frac{V_f^o}{kT}\left|\tau_g^o - x_g^o\right|\left\{1-\left[1+\left(\frac{\left|\tau_g^o - x_g^o\right|}{\tau^{Orowan}}\right)^s\right]^{-1/s}\right\}\right] \operatorname{sign}\left(\tau_g^o - x_g^o\right), \tag{2}$$

$$\tau^{Orowan} = \alpha \frac{K\, b}{\sqrt{3/2}\, w},$$

where the parameter s controls the degree of smoothness of the elastic-plastic transition, g is the (octahedral) slip system, ρ_g^o is the mobile dislocation density and x_g^o the kinematic hardening variable.

Rafting is assumed to be controlled by the difference of the dislocation densities between the vertical and the horizontal channels and the resulting distribution of internal stresses. In the frame of a macroscopic model, a detailed description of the dislocation distribution is not possible. Alternatively, the driving force for rafting X is assumed to be a measure of the kinematic hardening (see [5] [8] for details) and rafting progress is described by a phenomenological law with saturation

$$\dot{\xi} = (1-\xi)\, f^{raft}\, X^n. \tag{3}$$

Rafting completion, i.e. $\xi = 1$ and $w = w_{raft}$, corresponds to the ideal case of infinite plates (see equ. (1)). The model parameters f^{raft} and n have been estimated from direct measurements of the channel widths in crept specimens under several loadings. **Figure 14** shows an example of calculated and measured channel widths.

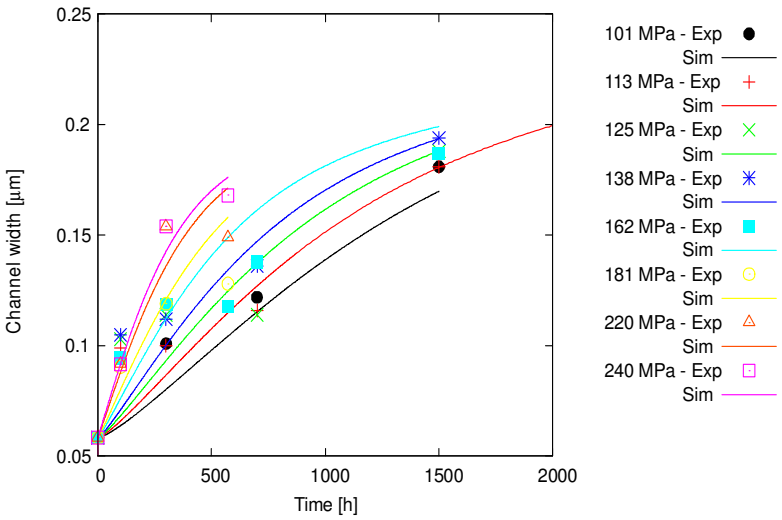

Figure 14: Evolution of the channel width during creep at 950°C for several load levels.

The remaining model parameters have been estimated from a large number of test results including monotonic tensile, cyclic, relaxation and creep tests in <001> and <111> specimens. As an example, **Figure 15** shows the comparison between model simulations and experiments for creep tests at 950°C with <001> specimens.

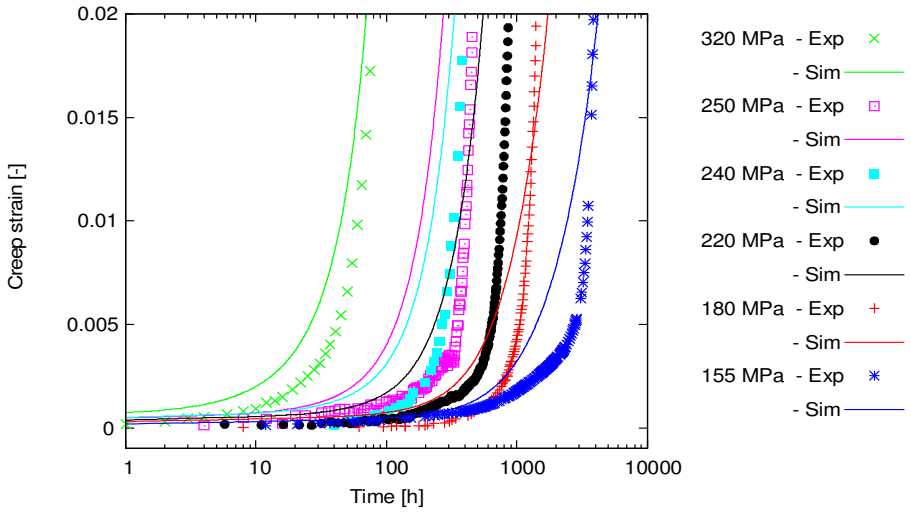

Figure 15: Simulation of creep tests at 950°C

The present model has been implemented in a UMAT subroutine for use with the FE program ABAQUS. An example of analysis of a complex loading condition is presented in section 5.

Finally, the ability of the model to describe the post-rafting mechanical behaviour has been assessed with mechanical tests on pre-crept, i.e. degraded specimens, under several conditions. In the case of a subsequent tension loading, the results are presented in **Figure 16** for several degradation conditions resulting in several final channel widths. The measured channel widths are indicated. It is clear that the tensile strength decreases as function of the channel width, a feature which is correctly captured by the model.

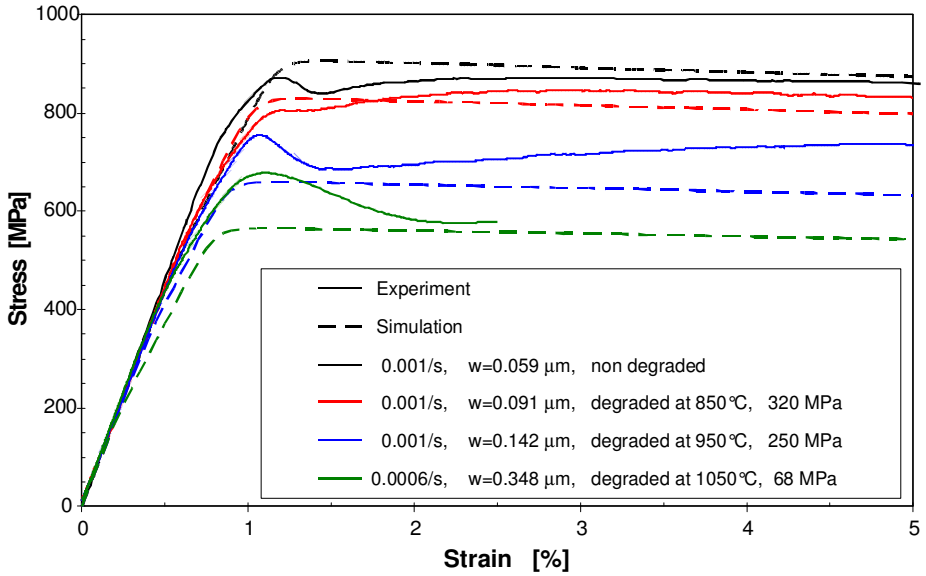

Figure 16: Influence of degradation on tensile strength.

4. NLR / NLDA Constitutive Material Model

In the NLR / NLDA approach, a multi-scale framework has been developed in which the different aspects of the Ni base superalloy behaviour are modelled [9] to [13]. The developed multi-scale model [10] for the prediction of the superalloy mechanical behaviour covers several length scales, as is shown schematically in **Figure 17a**. The macroscopic length scale characterises the engineering level on which a finite element (FE) model is commonly used to solve the governing equilibrium problem. The mesoscopic length scale represents the level of the microstructure within a macroscopic material point. At this length scale the material is considered as a compound of two different phases: γ'-precipitates embedded in a γ-matrix. Finally, the microscopic length scale reflects the crystallographic response of the individual material phases. The constitutive behaviour is defined on this level using a strain gradient crystal plasticity framework.

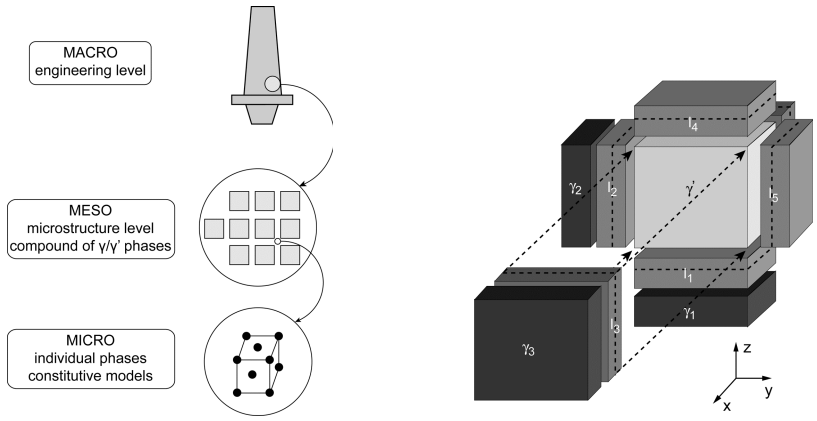

a) b)

Figure 17: Schematic overview of the model, showing (a) the multi-scale framework and (b) the multi-phase unit cell, consisting of one precipitate (γ'), three matrix (γ_i) and six double interface (I_i) regions.

On the material point level the Ni-base superalloy microstructure, consisting of γ'-precipitates in a γ-matrix, is represented by a unit cell containing 16 regions, see **Figure 17b**: one γ'-precipitate region, three γ-matrix channel regions with different orientations and 12 interface regions containing the γ/γ'-interfaces. The limited size of the unit cell and the micromechanical simplifications make the framework particularly efficient in a multiscale approach and is computationally much more efficient than a detailed FE based unit cell discretization.

The matrix phase constitutive behaviour is simulated by using a non-local strain gradient crystal plasticity model. In this model, non-uniform distributions of geometrically necessary dislocations (GNDs), induced by strain gradients in the interface regions, affect the hardening behaviour. The basic ingredient of the model is the relation between the slip rates $\dot{\gamma}$ and the resolved shear stresses τ^{α} for all the slip systems α. The following formulation is used:

$$\dot{\gamma} = \dot{\gamma}_0 F\left(\Omega^{\alpha}\right)\left\{\frac{\left|\tau^{\alpha}_{eff}\right|}{s^{\alpha}}\right\}^{m}\left\{1-\exp\left(-\frac{\left|\tau^{\alpha}_{eff}\right|}{\tau^{or}}\right)\right\}^{n} sign\left(\tau^{\alpha}_{eff}\right) \tag{4}$$

where τ^{or} denotes the Orowan stress, s^{α} the actual slip resistance and τ^{α}_{eff} the effective shear stress on slip system α, obtained from the effective stress tensor $\boldsymbol{\sigma}_{eff}$ using the symmetric Schmid tensor. The factor F is a cross slip factor that will be discussed below, while $\dot{\gamma}_0$, m and n are material constants.

The majority of the superalloy constitutive models available in literature contain, in addition to the octahedral systems, a set of cube slip systems to correctly simulate the material behaviour at orientations other than <001>, whereas experiments show that the

occurrence of macroscopic cube slip is quite exceptional. In the present model, the octahedral cross slip processes, that are physically responsible for the major part of the cube slip, are modelled and their effect is incorporated [11]. A parameter Ω^α is introduced to quantify the amount of cross slip. A higher value of Ω^α indicates a more favourable condition for cross slip. Therefore, a cross slip factor F based on the value of Ω^α is incorporated to enhance the slip rate of the slip systems:

$$F\left(\Omega^\alpha\right)=\left(C_{cs}\frac{\tau}{s^\alpha}\right)^{\varphi\left(\Omega^\alpha\right)} \quad \text{with} \quad \tau=\max\left(\tau_{eff}^\alpha,\tau_{cs}\right) \tag{5}$$

where $\varphi\left(\Omega^\alpha\right)$ quantifies the stress dependence of the cross slip, whereas C_{cs} and τ_{cs} are material constants.

The major part of plastic deformation is accommodated by the matrix phase, where dislocations are moving through relatively narrow channels. When encountering a precipitate, a loop is created around the particle, enabling the dislocation to continue its motion on the slip plane behind the precipitate. The dislocation loop around the precipitate may disappear by two different mechanisms, precipitate shearing or recovery climb, both involving inelastic deformation of the precipitate. These mechanisms are incorporated in the model [11], yielding the following slip law:

$$\dot{\gamma}^\alpha=\frac{SbS_{\mathrm{int}}}{V}\rho_{GND,\mathrm{min}}^\alpha\left[f_{diss}\left\{1-\exp\left(-\frac{\left|\tau_{eff}^\alpha\right|}{s_0^\alpha}\right)\right\}^p+\frac{4v_{c\lim b}^\alpha}{H_{\gamma'}}\left\{1-\exp\left(-\frac{\left|\tau_{eff}^\alpha\right|}{\tau_{cr}^\alpha}\right)\right\}\right]sign\left(\tau_{eff}^\alpha\right) \tag{6}$$

where S, S_{int}, V and H_γ are geometrical constants related to the dimensions of the microstructure. $\rho_{GND,\mathrm{min}}^\alpha$ represents the number of dislocations available for climb or shearing, v_{climb} is the climb velocity and f_{diss}, p and τ_{cr} are model parameters.

In addition to the model describing the material deformation, a damage model has been developed [12] that integrates time-dependent and cyclic damage into a generally applicable time incremental damage rule. The time dependent part of the damage rule is based on the model proposed by Levkovitch et al. [14], whereas the fatigue damage is attributed to irreversibility in the slip mechanism [15, 16]. This is incorporated in the model by introducing a criterion based on the Orowan stress to detect slip reversal on the microscopic level. The cyclic damage accumulation is quantified using the maximum values of resolved shear stress and slip rate during the "cycle". Also, the interaction between cyclic and time-dependent damage accumulation is incorporated in the model.

Finally, the rafting and coarsening processes are modelled by defining evolution equations for several of the microstructural dimensions [13] that are defined in **Figure 18**.

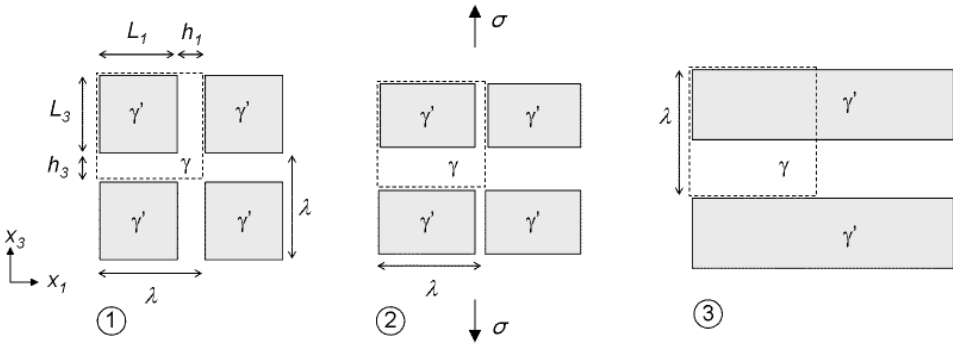

Figure 18: Schematic representation of the changes in microstructural dimensions at three different stages of the degradation process: 1) initial state; 2) microstructure in a rafted state; 3) fully rafted microstructure after a certain amount of coarsening.

The phenomenological relation for the horizontal channel widening rate $\dot{h}_i$ during vertical tensile loading as derived by Epishin et al. [4] was taken as the point of departure for the present model. However, the relation was extended to be applicable for a general multiaxial stress state. The evolution rate of the precipitate size ($\dot{L}_i$) is then given by:

$$\dot{L}_i(T,\sigma) = -\frac{3}{2} L_i \left[\frac{\sigma_{ii}^d}{\sigma_{VM} + \varepsilon} \right] \frac{A^*}{L} \exp\left[-\frac{Q - \sigma_{VM} U(T)}{RT} \right] \tag{7}$$

where σ_{ii} and σ_{VM} are the deviatoric and von Mises stress, respectively. The function *U(T)* defines the temperature dependence, whereas ε, A^* and Q are model parameters. In addition to the rafting, a formulation for the coarsening process is derived, quantifying the evolution of the microstructure periodicity λ, see **Figure 18**. Since the microstructural dimension are already part of the model, the effect of the microstructure degradation on the mechanical response of the material is almost automatically obtained.

The framework capabilities are demonstrated by applying the model to smooth CMSX-4 specimens that have been tested within the COST 538 Action. The predicted tensile response is compared to the experimental results in **Figure 19** for specimens with different degrees of degradation (characterized by the increasing channel width *h*). The model simulates these test quite well.

Finally, the fatigue lives of several test bars, both virgin and degraded, have been predicted. In **Figure 20** these values are compared to the experimentally obtained numbers of cycles to failure. The figure shows that only a few tests at 750°C are outside the factor-2 band, while the other tests could be simulated quite accurately.

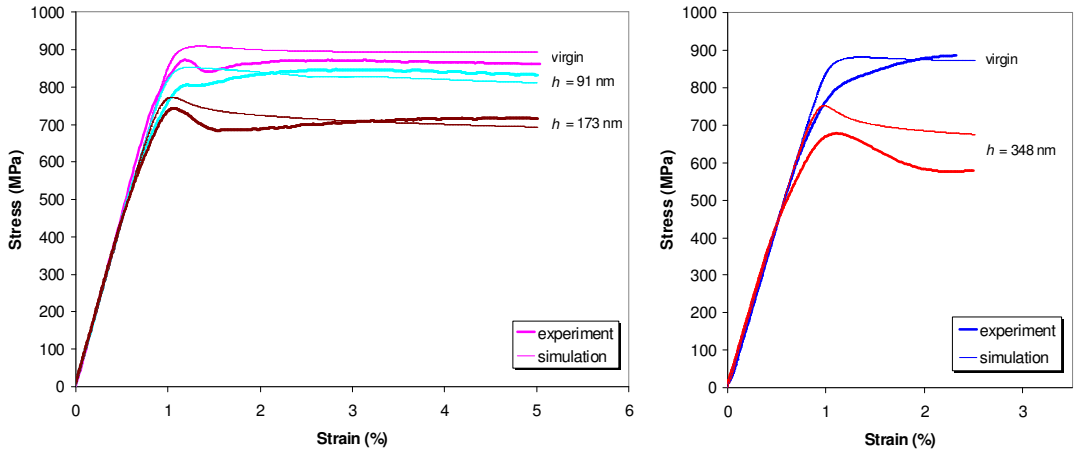

Figure 19: Simulated tensile tests at 950 °C and strain rates 10^{-3} s^{-1} (left) and $0.6 \cdot 10^{-3}$ s^{-1} (right) compared to experimental results for virgin material and different degrees of degradation [9].

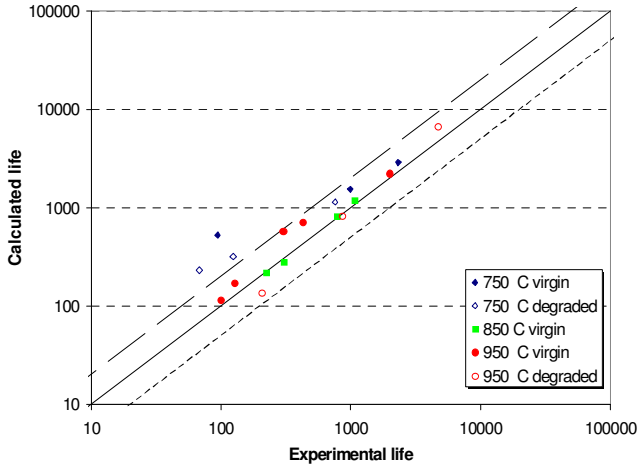

Figure 20: Calculated versus experimental life times using the damage model including the degradation mechanism [9].

5. Validation

For validation purposes, a limited number of notched specimens with K_t=1.41 in both as delivered and degraded conditions, were fatigue tested using stress control mode [1]. The results of this investigations are shown in **Figure 21**.

As an important validation step, the material models have been applied to Finite Element calculations in order to recalculate the stress strain distribution at notches under different loading situations. Details of calculation are available in the report [8]. In **Figure 22** the results of the simulation of rafting with the BAM constitutive model in a notched specimen at 950°C is presented and compared with SEM morphology observations after 1000h creep loading.

The calculated degree of rafting progress ξ defined in equ. (1) is shown to qualitatively agree with the observations.

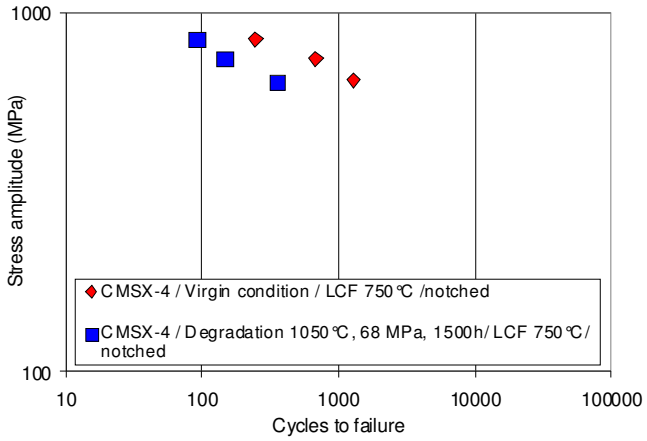

Figure 21: Influence of degradation on fatigue life at load controlled tests with notched specimens [1], CMSX-4 <001>

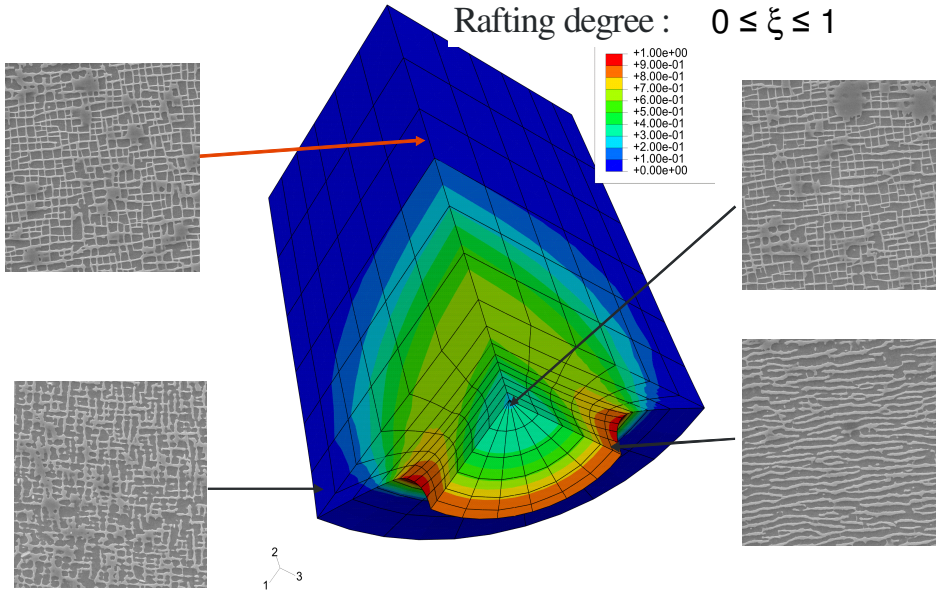

Figure 22: Simulation of rafting in a notched specimen crept at 950°C and comparison with the SEM observations after 1000h

6. Case Studies

Five ex-service blades of SX-CMSX-4 were supplied by SIEMENS Industrial Turbo-machinery Ltd, Lincoln, for mechanical and metallographic investigations. The following service conditions were reported for these blades:

Operation hours: 12,700
Number of starts: 200
Coating: Sermaloy 1515
Length of airfoil: 40mm
Temperature distribution in airfoil: Section 1: 807°C; Section 2: 927°C; Section 3: 997°C
Stress distribution : Section 1: 189MPa, Section 2: 111MPa, Section 3: 30MPa

The ex-service blade, the machined specimens, the distribution of temperatures and stresses along the airfoil (acc. to SIEMENS) are shown in **Figure 23**.

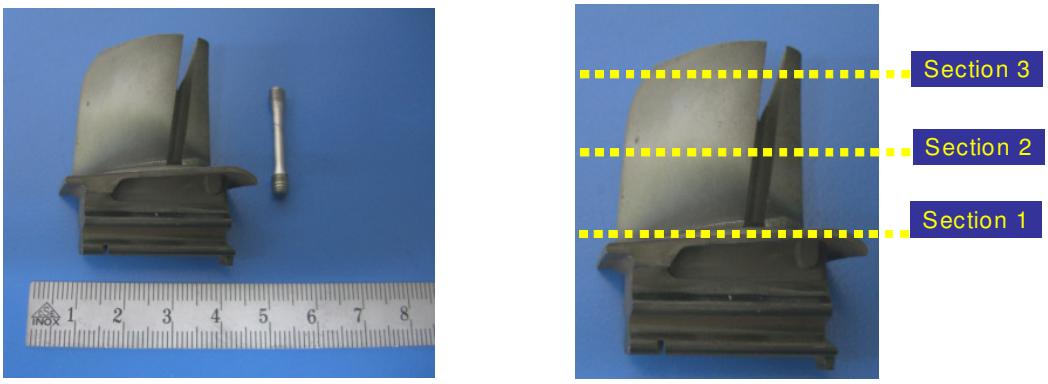

Figure 23: Ex-service blade and distribution of temperatures and stresses along the airfoil (reported by Siemens) [1]

From each blade a specimen was taken from the airfoil in order to perform tensile tests. Service loading led to a reduction in yield stress at room temperature as compared with that of the as-delivered conditions (**Figure 24**). At 800 and 850°C service loading also leads to a reduction in yield stress and corresponding rupture elongation (**Figure 25**). The microstructure of the ex-service blade as shown in **Figure 26**, illustrates the effect of long term high temperature exposure in inducing the changes in the morphology of γ/γ` phases.

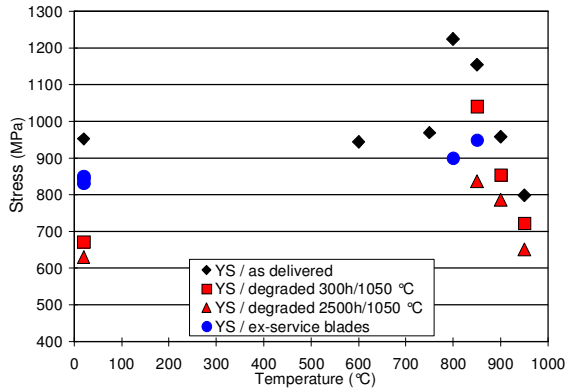

Figure 24: Influence of service loading on yield stress in comparison to as-delivered and degraded conditions, CMSX-4 <001>

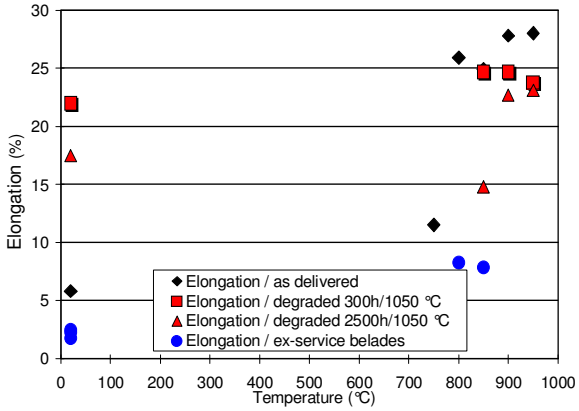

Figure 25: Influence of service loading on rupture elongation in comparison to as-delivered and degraded conditions, CMSX-4 <001>

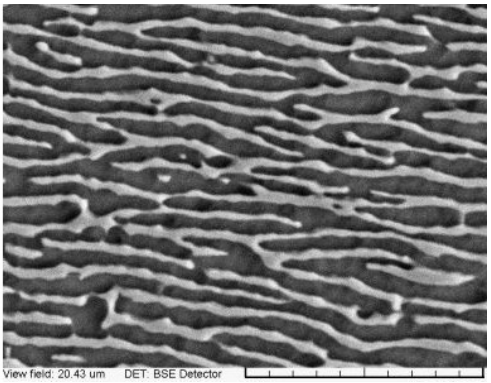

Figure 26: Microstructure of airfoil, ex-service blades CMSX-4

Simulation of microstructural evolution by NLR /NLDA model [9] on an internally and film cooled turbine blade can be compared with the results presented in [4]. The experimentally examined microstructure (**Figure 26**) at three different locations in an ex-service CMSX-4 (uncooled) turbine blade correspond to the results shown in the simulation (**Figure 27**). Here the almost virgin microstructure at the blade platform (Section 1) and the varying orientation of the rafts at the tip region (Section 3) nicely correspond to the results shown in **Figure 27**.

The fully rafted microstructure at the blade centre was not observed here for two reasons: the simulated duration of 1,000hrs is much shorter than the 12,700 hrs in [4], and the internal blade cooling yields much lower temperatures in the centre region of the blade, which reduces the degradation rate there. These results clearly demonstrate that the typical case of a material loaded uniaxially in radial direction, which is mostly studied in literature, is not representative for most of the locations in this real component. That is especially due to the fact that the present blade is internally cooled, resulting in thermal stresses that cause the stress state to be multiaxial.

Concurrent with the microstructure degradation, the creep deformation of the blade is calculated. The results indicate that the high creep strain regions at the suction side of the blade are hardly affected by the degradation. Moreover, the maximum value of the creep strain, located at the inner surface of the blade in one of the cooling channels, has decreased slightly from $1.30 \cdot 10^{-3}$ m/m in the virgin blade to $1.27 \cdot 10^{-3}$ m/m in the degraded blade. However, the equivalent creep strain near the tip at the pressure side is much higher in the degraded blade than in the virgin blade. The evolution of the creep strain at this location is plotted in **Figure 28** for both the virgin and the degraded blade, showing a significant increase in the creep rate.

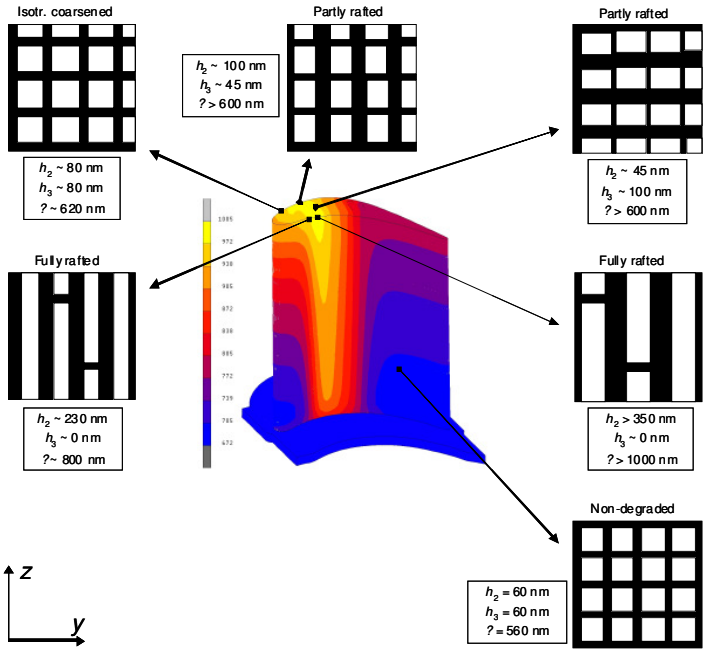

Figure 27: Overview of degraded microstructures observed after a simulation of degradation in a cooled turbine blade under service conditions for 1000 hours. The contours indicate the blade temperature distribution

These results demonstrate that the effect of degradation on the overall creep deformation is rather limited for this specific component, so the blade elongation is hardly affected by the degradation. However, local creep strain rates, especially in the hot regions of the blade, considerably increase after degradation. Neglecting the effects of rafting and

coarsening in the numerical analysis would thus lead to non-conservative life predictions. This clearly demonstrates the benefit of a model that includes the effects of degradation.

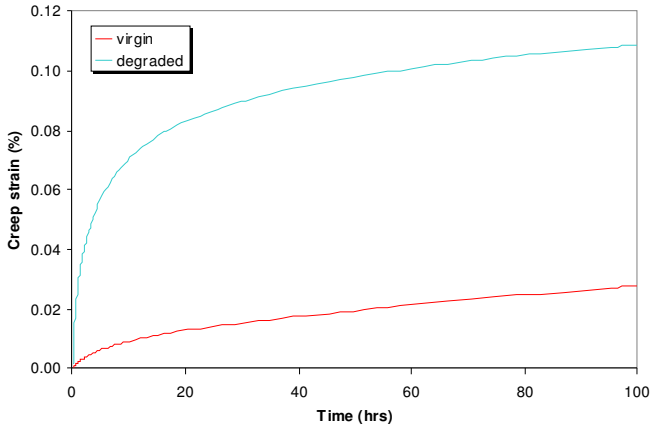

Figure 28: Comparison of the equivalent creep strain evolution in a virgin and a degraded blade for a specific location at the blade tip [9]

7. Conclusions

Different models on the effect of microstructural changes due to degradation have been developed. The effect of microstructural degradation on tensile and low cycle fatigue properties and at different temperatures has been determined and correlated to the microstructure based models. The two lifetime models, based on different concepts, were developed including the degradation effect on microstructure. Both models were successfully applied to simulate the tensile, creep and low cycle fatigue behaviour of degraded material. The application is limited to a temperature range of 950°C. In terms of validation notched fatigue data at two different temperatures i.e.750 and 950°C were considered. The developed microstructural models have been successfully applied to an ex-service un-cooled blade i.e. a case study.

8. Acknowledgement

The authors thank Howmet, Exeter for providing the test materials. Financial support of Deutsche Forschungsgemeinschaft, Swiss State Secretariat for Education and Research SER and Netherlands Ministry of Defence is highly appreciated.

9. References

[1] Nazmy, M., M. Staubli and A. Künzler, Evaluation of Microstructural & Property Changes of Ni-Base Superalloys after High Temperature Creep Loading and its Rejuvenation, *COST 538, Final Report* (2004-2008).

[2] Scholz, A., Y. Wang, S. Linn, C. Berger and R. Znajda, Modelling of Mechanical Properties of Alloy CMSX-4, *Materials Science and Engineering*, A 510-511 (2009), 278-283

[3] Nazmy, M., A. Epishin, T. Link, M. Staubli: Degradation In Single Crystal Nickel-Superalloys – A Review, in "Materials For Advanced Power Engineering 2006", Eds. J. Lecomte-Beckers, et. al., *Proc. of the COST Conf.*, Liège 18 – 20 Sept. (2006), 205-216.

[4] Epishin, A., T. Link, M. Nazmy, M. Staubli, H. Klingelhoeffer and G. Nolze: Micro-structural Degradation of CMSX-4: Kinetics and Effect on Mechanical Properties, Super-alloys 2008", Eds. R.C. Reed et. al., *The Minerals, Metals & Materials Society*, 725-731, 20.

[5] Fedelich, B., G. Künecke: Modelling the Microstructural Degradation of the alloy CMSX-4 under High Temperature Loading and its Influence on the Mechanical Behaviour, *COST 538 Final Report*, BAM (2008).

[6] Epishin, A., T. Link, H. Klingelhoffer, B. Fedelich, U. Bruckner, P. D. Portella: New technique for characterization of microstructural degradation under creep: Application to the nickel-base superalloy CMSX-4, *Materials Science and Engineering* A 510–511 (2009), 262–265.

[7] Scholz, A.: Modelling of Microstructural and Mechanical Property Changes in Gas Turbine Alloys, COST 538 Final Task Leader Report, TU Darmstadt (2008)

[8] Fedelich, B., G. Künecke, A. Epishin, T. Link and P. D. Portella: Constitutive modelling of creep degradation due to rafting in single-crystalline Ni-base superalloys, *Materials Science and Engineering* A 510-511 (2009), 273/277.

[9] R. Huls, T. Tinga: Multi-scale Modelling of SX superalloys, *COST 538 Final Report* (NLR) 2008

[10] Tinga, T., W. A. M. Brekelmans, and M. G. D. Geers, Incorporating strain-gradient effects in a multi-scale constitutive framework for nickel-base superalloys, *Philosophical Magazine* 88, 30-32 (2008), 3793-3825.

[11] Tinga, T., W. A. M. Brekelmans, and M. G. D. Geers, Cube slip and non-Schmid effects in single crystal nickel-base superalloys, Modelling and Simulation in Materials Science and Engineering 18(015005) (2010), 1-31.

[12] Tinga, T., W. A. M. Brekelmans, and M. G. D. Geers, Time-incremental creep-fatigue damage rule for single crystal Ni-base superalloys, *Materials Science and Engineering* A 508 (2009), 200-208.

[13] Tinga, T., W. A. M. Brekelmans, and M. G. D. Geers, Directional coarsening in nickel-base superalloys and its effect on mechanical properties, *Computational Materials Science* 47 (2009), 471-481.

[14] Levkovitch, V., R. Sievert, and B. Svendsen, Simulation of deformation and lifetime behavior of a fcc single crystal superalloy at high temperature under low-cycle fatigue loading, *International Journal of Fatigue*, 28 (2006), 1791-1802.

[15] Shyam, A. and W. W. Milligan, A model for slip irreversibility, and its effect on the fatigue crack propagation threshold in a nickel-base superalloy, *Acta Materialia*, 53 (2005), 835-844.

[16] Fedelich, B., A microstructural model for the monotonic and the cyclic mechanical behavior of single crystals of superalloys at high temperatures, *International Journal of Plasticity* 18 (2002), 1-49.